Functional magnetic resonance imaging of the human brain

Seong-Gi Kim *, Kamil Ugurbil

Center for Magnetic Resonance Research, Department of Radiology, University of Minnesota Medical School, 385 East River Road, Minneapolis, MN 55455, USA

Abstract

The current technical and methodological status of functional magnetic resonance imaging (fMRI) is reviewed. The mechanisms underlying the effects of deoxyhemoglobin concentration and cerebral blood flow changes are discussed, and methods for monitoring these changes are described and compared. Methods for post-processing fMRI data are outlined. Potential problems and solutions related to vessels and motion are discussed in detail. © 1997 Elsevier Science B.V.

Keywords: Brain mapping; Functional imaging; Functional MRI; Cortical mapping

1. Introduction

The idea that regional cerebral blood flow (rCBF) could reflect neuronal activity began with the experiments of Roy et al. (1890). This concept is the basis for many of the functional imaging techniques being used today. The focal increases in rCBF as measured by radioactive Xe or positron emission tomography (PET) are considered to reflect local neural activity (see Raichle, 1987). Traditionally, magnetic resonance imaging (MRI) (Lauterbur, 1973) of the human brain has been used mainly to study neuroanatomy and neuropathology. However, recent developments (Ogawa et al., 1990a; Ogawa and Lee, 1990; Ogawa et al., 1990b) permitted the extension of MRI techniques to visualization of human brain function.

In 1990, Ogawa and colleagues at AT and T Bell Laboratories (Ogawa et al., 1990a; Ogawa and Lee, 1990; Ogawa et al., 1990b) reported the blood oxygenation level dependent (BOLD) contrast mechanism for magnetic resonance imaging; they demonstrated that in conventional gradient-recalled echo MR images of rat brains, signals from venous vessels can be modulated by pharmacologically-induced changes in CBF and oxygen utilization as a consequence of altered blood deoxyhemoglobin content. Subsequently, Turner et al. (1991) at the National Institutes of Health acquired fast echo planar images (EPI; Mansfield, 1977) to investigate the time course of blood oxygenation in cat brain during the course of anoxia, demonstrating progressively decreasing signal intensity reflecting increasing deoxyhemoglobin concentration following the onset of anoxia (Turner et al., 1991). These early animal studies suggested the possibility of functional mapping of the human brain using BOLD contrast.

The first human task-induced functional imaging study was performed using an exogenous paramagnetic contrast agent, gadolinium diethylene-triamine-penta-acetic acid (Gd-DTPA) which remains intravascular in the brain in the presence of an intact blood brain barrier (Belliveau et al., 1991). Following a bolus administration of Gd-DTPA, gradient-echo EPI signal from vessels and surrounding tissue areas decreases during the first passage. By integrating over the first passage of the contrast agent, cerebral blood volume (CBV) can be determined (Rosen et al., 1991). Using this technique, an increase of CBV in the human visual cortex was observed successfully during visual stimulation (Belliveau et al., 1991). This demonstrated that MRI can detect small signal changes induced by neuronal activity in the human brain.

* Corresponding author. Tel.: +1 612 6267007; fax: +1 612 6267005; e-mail: kim@geronimo.drad.umn.edu

Papers reporting the first successful use of the BOLD contrast to generate functional maps of the human brain with MRI, without the use of exogenous contrast agents, were submitted for publication within 5 days of each other in 1992 by groups in the University of Minnesota working with AT and T Laboratories (Ogawa et al., 1992), Massachusetts General Hospital (Kwong et al., 1992), and the Medical College of Wisconsin (Bandettini et al., 1992). Since then, fMRI has been successfully performed in many laboratories with both high magnetic fields (e.g., Menon et al., 1992; Kim et al., 1993a,b; Hinke et al., 1993; Turner et al., 1993) and magnetic fields available in clinical scanners (e.g., Frahm et al., 1992; Blamire et al., 1992; Constable et al., 1993; Connelly et al., 1993), as well as with either conventional gradient recalled echo sequences (e.g., Menon et al., 1992; Frahm et al., 1992; Kim et al., 1993a,b; Hinke et al., 1993; Constable et al., 1993; Connelly et al., 1993) or echo-planar imaging (e.g., Blamire et al., 1992; Turner et al., 1993).

BOLD-based fMRI opened a new era of visualizing functional activity in the human brain (Kim et al., 1993a,b; Rao et al., 1993; Schneider et al., 1993; Ellermann et al., 1994; Kim et al., 1994b; McCarthy et al., 1993; Karni et al., 1995; Sane et al., 1995; Shaywitz et al., 1995; Sereno et al., 1995). fMRI provides advantages over other functional mapping modalities such as single photon emission computed tomography (SPECT) and PET: (i) MR functional imaging has in principle considerably higher spatial and temporal resolution. (ii) fMRI procedures are completely non-invasive and can be repeated in a single subject without concern for exposure to ionizing radiation. (iii) Since anatomic and functional images can be acquired during the same imaging session, functional maps can be compared directly with anatomic images without any misregistration.

In this article, the current technical and methodological status of fMRI is summarized. Underlying mechanisms of BOLD effects, and data collection and post-processing methods are reviewed. Potential problems and solutions related to vessels and motion are discussed in detail.

2. BOLD-based fMRI

2.1. Mechanisms

The basis of the BOLD technique is the fact that deoxyhemoglobin acts as nature's own intravascular paramagnetic contrast agent (Pauling and Coryell, 1936; Thulborn et al., 1982; Ogawa et al., 1990a; Ogawa and Lee, 1990; Ogawa et al., 1990b). When placed in a magnetic field, deoxyhemoglobin alters the magnetic field in its vicinity, particularly when it is compartmentalized as it is within red blood cells and within the vasculature. The effect increases as the concentration of deoxyhemoglobin increases. At concentrations found in venous blood vessels, a detectable local distortion of the magnetic field surrounding the red blood cells and surrounding blood vessel is produced. This affects the magnetic resonance behavior of the water proton nuclei (which are used for MRI) within and surrounding the vessels, which in turn result in decreases in both the transverse relaxation time (T_2) (Thulborn et al., 1982; Ogawa et al., 1993b) and the apparent transverse relaxation time (T_2^*) (Ogawa et al., 1990a; Ogawa and Lee, 1990; Ogawa et al., 1990b), and thus attenuating signal intensity in T_2^* and T_2-weighted MR images.

The concentration change of deoxyhemoglobin (leading to BOLD effect) due to neuronal activity was examined by optical spectroscopy in animals and PET in humans. Oxyhemoglobin, deoxyhemoglobin and cerebral blood volume can be detected by near infrared spectroscopy; absorption at the different frequencies can provide various physiological information. Grinvald et al. (1991) studied hemodynamic changes of the visual area in an awake monkey during visual stimulation; two different phases of deoxyhemoglobin concentration changes were observed. Following the onset of visual stimulation, oxygen consumption (OC) is increased rapidly while elevation in CBF lags behind, thus resulting in an increase in deoxyhemoglobin content that peaks at about 2.5 s after the start of visual stimulation. This initial response must occur when electrical activity and hence cellular metabolism is elevated. During this period, a negative BOLD signal change would be expected. Subsequently, the increase in CBF and O_2 delivery to the tissue exceeds the extraction by the elevated OC, resulting in a reduction of the deoxyhemoglobin content. This later hemodynamic response covers a larger area compared to the initial response (Frostig et al., 1990; Grinvald et al., 1991). Uncoupling between CBF and OC was also reported in humans by PET studies during visual and somatosensory stimulation (Fox and Raichle, 1986; Fox et al., 1988). This mismatch results in an increase in the signal intensity of T_2^*- and T_2-weighted MR images.

To examine whether changes in BOLD-based fMRI signal correlate with optical responses based on intrinsic signals, Menon et al. (1995a) have studied temporal responses of MR signal during visual stimulation at 4 Tesla, using EPI with a temporal resolution of 100 ms. They found two distinct areas in the visual cortex with different hemodynamic responses; one area had only a slow but large magnitude ($\sim 6\%$) positive change, and the other area, which covered $\sim 30\%$ of the total region that responded to the visual stimulation, showed a rapid initial negative change ($\sim 1\%$). These negative signal changes were observed during the first 0.5–2.5 s

of photic stimulation followed by a reversal in signal intensity that reached a peak positive signal changes of $\sim 2\%$ relative to the basal pre-stimulation state at about 5 s after the beginning of the visual stimulation. The areas with negative dips did not lie in large vessels. This observation is consistent with previous optical studies of deoxyhemoglobin concentration change (Grinvald et al., 1991), suggesting that fMRI signal originates from changes of deoxyhemoglobin content. Using proton spectroscopy with spatial resolution of $2 \times 2 \times 2$ cm³, Ernst and Hennig (1994) showed a negative signal change of 0.25% at 500 ms after a very brief visual stimulation, but this change may not have been due to the BOLD effect since it disappeared at longer gradient echo times which would have enhanced the BOLD contrast (Hennig et al., 1995).

2.2. Techniques

To acquire data for an image with a $N \times M$ matrix size, a 'readout' data set with N points that encodes spatial information in one direction is collected M times with incremental increase of the 'phase-encoding' gradient that encodes spatial information in a second, orthogonal direction. Then, an image with a $N \times M$ matrix size is constructed by 2-D Fourier-transformation. Nominal spatial resolution of the image is determined by the 'field of view' divided by matrix size. For example, a 20 cm field of view and 64 data points give a spatial resolution of 3.1 mm, provided that a post-acquisition data manipulation that degenerates resolution, such as 'filtering' for improved signal-to-noise ratio (SNR), has not been performed. There are two major types of MR imaging techniques used for functional brain mapping; one is based on conventional methods, and the other uses high speed approaches such as EPI. For conventional images, each readout data set with N points is acquired after each radio frequency (RF) excitation pulse and this process is repeated for each phase-encoding step required. For example, when an image with a 64×64 matrix size is obtained with a repetition time (TR) of 50 ms between each phase encoding step, the total imaging time is 3.2 s. In contrast, with EPI images (for a review, see Stehling et al., 1991), each readout data set with N points is acquired repeatedly and consecutively by oscillating the readout gradients (with incremental increase in the phase-encoding gradients during each reversal) following a single RF pulse. Thus, the acquisition time for a single image is extremely short (approximately 30–100 ms).

The most common conventional fMRI technique is a fast low angle shot (FLASH; Haase et al., 1986) technique which we would refer to as 'conventional' since each phase encoding step follows an RF excitation. The imaging time is typically 2–10 s depending on matrix size of the image. The major advantage of FLASH is its

high spatial resolution. Using FLASH, Frahm et al. (1993) obtained high resolution functional activation maps during visual stimulation; fMRI with a voxel size as small as 2.5 μl were successfully acquired. With in-plane resolution of 1.25×1.25 mm², activation can be detected even in deep nuclei (Kim et al., 1994b). Fig. 1 shows a functional activation map overlaid on the T_2^*-weighted image of the cerebellum during performance of a cognitive puzzle task (Kim et al., 1994b). The dentate nuclei appear as dark areas in the middle of the cerebellum due to iron deposits. Only by using high spatial resolution can BOLD signal changes be observed within the dentate nuclei. This has not been possible by other mapping techniques such as PET. An additional advantage of conventional techniques with high resolution is the ability to identify large venous vessels. Since venous vessels have short T_2^* due to high deoxyhemoglobin concentration, they appear as dark lines or spots in high resolution T_2^*-weighted images (Menon et al., 1993; Kim et al., 1994a). This helps to avoid ambiguities by allowing the assignment of changes in functional maps to the underlying tissue structure. Disadvantages of conventional techniques are long acquisition times and a high sensitivity to various types of motion (discussed in greater detail later). Since the acquisition of a single slice takes a long time, it is difficult to acquire an image of the whole brain during a functional imaging study.

To shorten the imaging time without using EPI, alternative techniques have been proposed (Moonen et al., 1992; Hu and Kim, 1993). For example, an 'echo-shifted' gradient-recalled echo imaging sequence, which increases the effective echo time without increasing the repetition time, was proposed by Moonen et al. (1992). This technique is relatively demanding on gradient strength and stability. Based on a magnetization prepared ultrafast gradient-recalled echo sequence (i.e., Turbo-FLASH; Haase, 1990), a T_2^*-weighted imaging technique was developed (Hu and Kim, 1993). One of the advantages of Turbo-FLASH is substantial suppression of flowing spins; this is desirable for fMRI. The major drawback of the technique is that the signal-to-noise ratio is reduced by a factor of 2 relative to an equal bandwidth FLASH sequence, and even more so relative to the currently-used low bandwidth FLASH.

EPI allows faster dynamic tracking of the functional activation, as fast as every 50 ms. This has applications in determining the time course of the hemodynamic responses (Menon et al., 1995a; see later). In fact, with EPI images, time resolution in functional studies is limited not by MR imaging but the hemodynamic response time in the brain which is approximately 3–6 s. During this response time, many images can be acquired in a single slice or in many slices. When a single slice is repeated rapidly, signal   a steady state condition, losing signal intensity and also leading
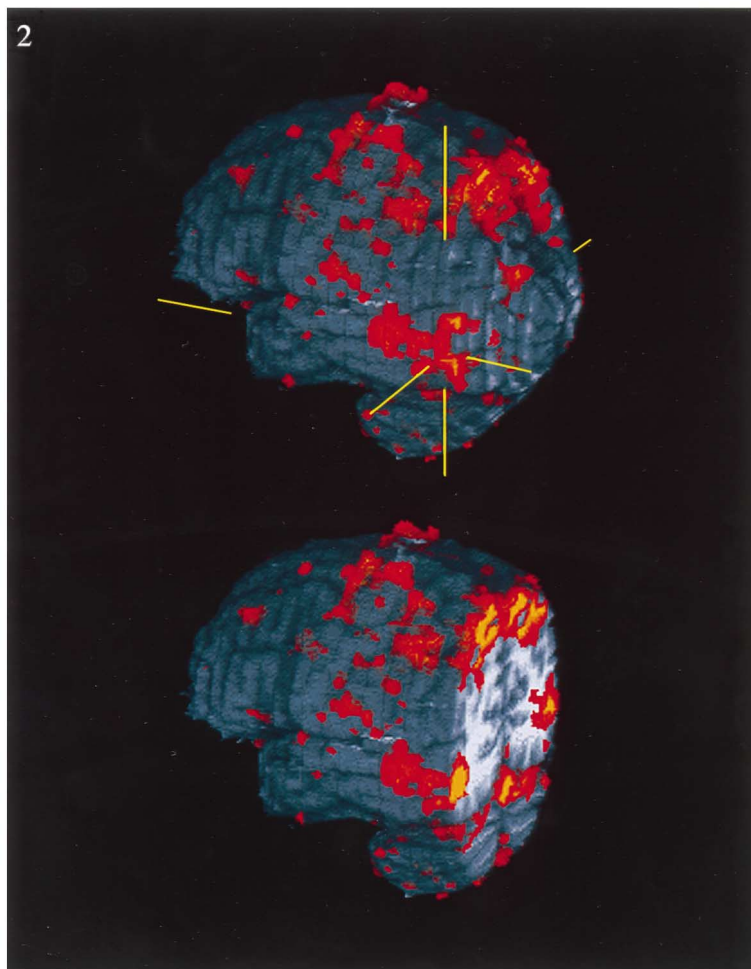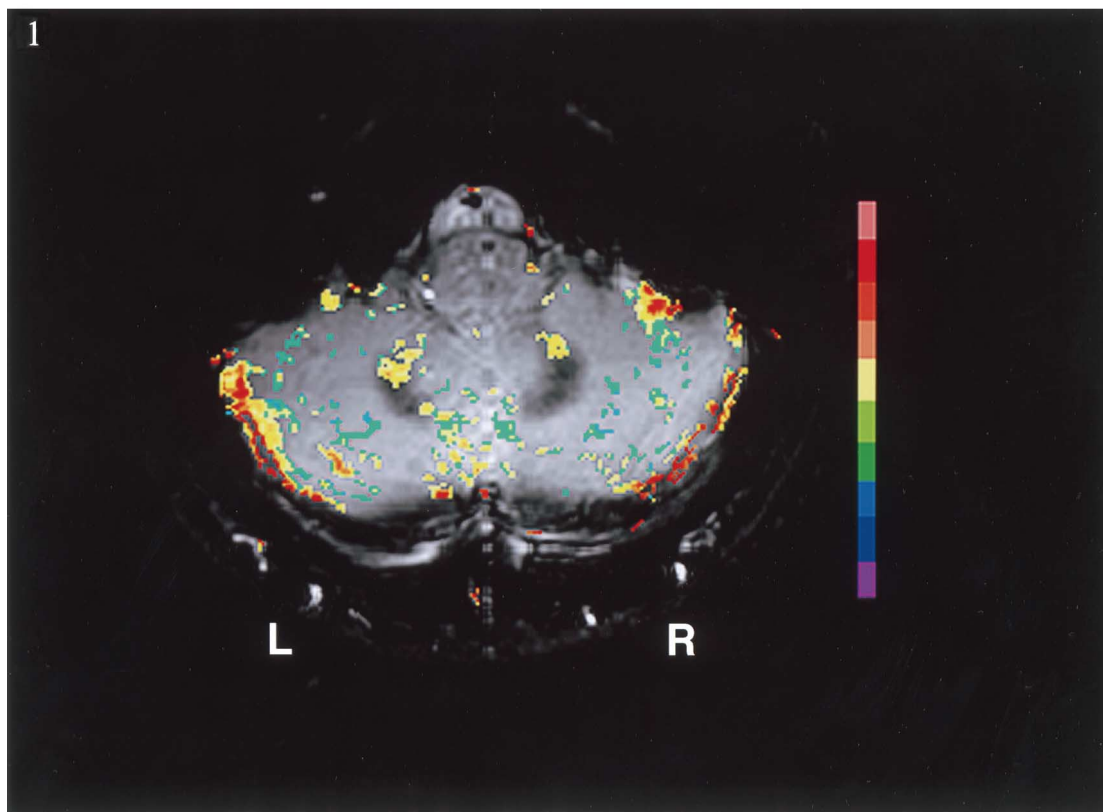
Fig. 1 and Fig. 2.

to sensitivity to inflow effects (see later). The speed of EPI can be used advantageously for other purposes: multislice images from the whole brain ('image set') can be acquired on the order of seconds. A larger number of image sets can be collected during paradigms, providing higher statistical power to determine activation maps. Signal fluctuations due to physiological processes can be captured accurately in time for post-acquisition data processing and possible elimination (discussed later). Thus, the ability to image rapidly is an important factor in functional imaging, particularly for multi-slice applications.

Fig. 2 demonstrates an fMRI study from the whole brain during performance of a visuo-motor error detection and correction task. Functional images were acquired with multi-slice EPI using a spatial resolution of $3.1 \times 3.1 \times 5$ mm^3 and a temporal resolution of 3.5 s. A 3-D image was reconstructed from the multi-slice 2-D images. A functional image of the whole brain (in color) was overlaid on anatomic images (in gray scale) and rendered using Voxel View software (Vital Images, Fairfield, Iowa). In this 3-D view, the activation areas seen are those on the outer cortical surface (mainly gyri) except when the image was 'cut', exposing the convolutions of the cortex and deep nuclei. The task consisted of visual presentation of a target on a screen and movement of a cursor from the center to the circumferential target using a joystick (Flament et al., 1997). During joystick movements, continuous error detection and correction is required. Activation was observed in many regions including motor, premotor and supplementary motor areas, prefrontal cortex, parietal cortex, thalamus and associative visual cortex including the MT region which is marked approximately by the intersecting lines in the whole brain image. The image was then 'cut' at the plane defined by two of these lines, exposing the extent of MT activation beyond the cortical surface (Fig. 2). Clearly, EPI or a similarly fast method is the choice of method for whole brain mapping. Additional advantages of the EPI technique is that spin-echo, asymmetric spin-echo and inversion recovery contrasts can be implemented easily.

Major problems of the EPI technique are that (i) single-shot EPI images may not yield activation maps with high spatial resolution, and (ii) the geometric distortions inherent in EPI make it difficult to accurately overlay EPI activation maps on conventional MRI images. Spatial resolution in EPI imaging can be improved using a multi-segment imaging technique (Rzedzian and Pykett, 1987; Butts et al., 1994; Kim et al., 1996). The image distortion of EPI is dependent on local magnetic susceptibility variations. Thus, this distortion is pronounced in areas with tissue-air interface such as the sinus areas, especially at higher magnetic fields because the susceptibility effect is proportional to the magnetic field strength. In some areas such as the frontal and temporal lobes, EPI-based fMRI may not be directly overlaid on the conventional anatomic images. This problem can be avoided by using the same pulse sequence and gradient strength for EPI and functional images, and thus distortion will be the same in both (Kim et al., 1996). However, eventually, correction needs to be done because of comparison with conventional images and standard brain atlases (Talairach and Tournoux, 1988). This correction can be done by magnetic field (i.e., susceptibility) mapping (Jezzard and Balaban, 1995) or other schemes (Bowtell et al., 1994).

For the present, conventional imaging techniques hold an edge over EPI with regard to spatial resolution, and EPI is preferable when mapping whole brain is desired. Conventional imaging techniques are more susceptible to motions, and echo planar images are more sensitive to geometric distortions.

3. Perfusion-based fMRI

Despite the ubiquitous use of BOLD-based techniques, the approach has some shortcomings. (i) BOLD effects are related to multiple physiological parameters such as CBF, CBV and OC; thus, it is virtually impossible to extract a single physiological parameter from the observed signal changes. (ii) Uncoupling between CBF and OC is the basis of BOLD fMRI; however, this

---

Fig. 1. Functional map (in color) in the cerebellum during performance of a cognitive peg-board puzzle task, overlaid on a T_2^*-weighted axial image in gray scale. The dentate nuclei appear as dark crescent shapes at the middle of the cerebellum due to iron deposits. fMRI images were acquired by conventional T_2^*-weighted FLASH techniques with a spatial resolution of $1.25 \times 1.25 \times 8$ mm^3 and a temporal resolution of 8 s. Each color represents a 1% increment, starting at 1%. R, right cerebellum; L, left cerebellum. A left-handed subject used the left hand to perform the task. Bilateral activation in the dentate nuclei and cerebellar cortex was observed. The activated area in the dentate nuclei during performance of pegboard puzzle was 3–4 times greater than that seen during the visually guided peg movements. (see details in Kim et al., 1994b).

Fig. 2. Whole brain functional imaging study during a visuo-motor error detection and correction task. Functional images were acquired by the multi-slice single-shot EPI imaging technique with spatial resolution of $3.1 \times 3.1 \times 5$ mm^3 and temporal resolution of 3.5 s. The skull and associated muscles were eliminated by image segmentation. The 3-D image constructed from multi-slice images was rendered by Voxel View program (Vital Images, Fairfield, Iowa). The task was to move a cursor from the central start box onto a square target by moving a joystick. Eight targets were arranged circumferentially at 45° angles and displaced radially at 20° around a central start box. Activation (in color) is observed at various brain areas. Top image displays the brain as a 3-D solid object so that only the cortical surface is seen. In the bottom image, a posterior section was removed at the level of the associative visual cortex to display activation not visible from the surface   provided by Jutta Ellermann, Jeol Seagal, and Timothy Ebner).

may not be valid under all circumstances and in all regions of the brain (Roland et al., 1987; Seitz and Roland, 1992). The potential problems can be overcome by alternative CBF or CBV-based MRI techniques.

As previously mentioned, an exogenous contrast agent was used to determine CBV changes during neuronal activity (Belliveau et al., 1991). However, the use of this technique is severely limited because of the need for repeated bolus injections of an exogenous contrast agent, and the necessity to compare images acquired during two different administrations of the contrast agent bolus separated by a relatively long period (several min).

Detre et al. (1992) reported an endogenous spin tagging technique, which uses endogenous blood water spins as a flow tracer. Spin tagging of blood water is achieved by the continuous inversion (or saturation) of flowing spins of the blood at the carotid artery in the neck. Tagged blood spins move into the imaging slice and exchange with tissue water spins, resulting in signal reduction in the imaging slice. This effect is directly related to CBF. Absolute CBF can be determined by correcting for the relaxation of tagged blood spins during the transit from carotid artery to the region of interest, together with the longitudinal relaxation time of tissues (T_1; which is also used for anatomic contrast). This technique was validated using hypercapnia in rats (Detre et al., 1992; Williams et al., 1992). In humans, the transit time of spins from the carotid artery to the tissue at the imaging slice will be long (~ 1 s) (Roberts et al., 1994), thus leading to loss of the 'tagging'. Furthermore, the technique can result in high power deposition at high magnetic fields. Therefore, this technique has not been successfully applied for fMRI studies in humans.

A slice-selective inversion recovery (IR)-based functional imaging technique has been used to map visual stimulation in the brain (Kwong et al., 1992). Following slice-selective inversion of the imaging slice, completely relaxed blood water spins from outside of the imaging slice move into the imaging slice and exchange with tissue water spins. This effect enhances signal intensities in the perfused areas and the enhancement becomes greater locally due to the task induced regional blood flow increase. This technique can determine the magnitude of the change in flow, but it does not have the potential for measurements of relative flow changes. In addition, since the flow-based techniques are most successful with fast imaging methods such as EPI, they in principle contain confounding effects from BOLD because of the inherent and inevitable T_2^* weighting present in EPI images; in the IR method used by Kwong et al. (1992), this BOLD contribution is not separable from the flow effects.

Edelman et al. (1994) have reported a flow technique based on echo-planar imaging and signal targeting with alternating radio frequency (EPISTAR), in which two images are acquired with and without spin tagging. The tagging inversion pulse is applied to the inferior area of the slice of interest which has an axial orientation. Since the imaging slice is saturated, signal in this area relies on longitudinal relaxation. With spin tagging, signal in the imaging slice will decrease due to the flow component (as seen in the Detre's method). By contrast, without spin tagging, the signal will increase because inflowing spins are fully relaxed (as seen in the slice-selective inversion method). The difference between the two images is directly related to CBF. Focal signal changes during motor and visual tasks were reported with this method (Edelman et al., 1994). This technique is sensitive to the T_1 of blood because, subsequent to spin 'tagging' (i.e., inversion) below the axial slice of interest, the tag is partly lost by T_1 relaxation while spins travel into the imaging slice. Thus, the exact relationship between percent signal changes in the images and alterations in blood flow is not straight forward (Edelman et al., 1994).

Recently, relative cerebral blood flow (relCBF) changes during increased neuronal activity have been measured quantitatively by a flow-sensitive alternating inversion recovery (FAIR) technique (Kim, 1995). In this method, two IR images are acquired consecutively; one uses slice-selective inversion, and the other uses non-slice selective, global inversion. During an inversion delay following the slice-selective inversion, fully magnetized blood spins move into the imaging slice due to blood flow and exchange with tissue water leading to blood flow dependent recovery of the initially inverted magnetization within the slice. However, in an image where the inversion pulse is global, this flow component is absent. Thus, signal difference between the two IR images is directly related to blood flow. Relative signal changes in the difference images during task periods represent relative changes in CBF (relCBF) (Kim, 1995). Also, absolute CBF changes can be determined because slice-selective IR images are acquired (Kwong et al., 1992). This technique was successfully applied to motor studies. A further advantage of this technique is the ability to separate flow effects from BOLD effects (Kim, 1995). This relCBF measurement by MRI is similar to the relCBF measurement technique by PET. The PET technique involves injection of $H_2^{15}O$ tracer and the counts of positron emission separately for two different experimental conditions; one during control and the other during task periods. Then, the ratio of the positron count is calculated on a pixel-by-pixel basis, which is the relative blood flow. Although the FAIR technique provides the same relCBF as PET, the MR method provides advantages due to availability of higher resolution in the MR method,

ease of use and absence of any invasive procedures. The imaging time of the FAIR technique can also be shorter than that of PET based relCBF measurements which need an inter-experiment delay in addition to data acquisition due to the half-life of ^{15}O (123 s).

One important advantage of CBF-based techniques is the ability to separate large and small vessel contributions by adjusting the delay time between spin tagging and detection. Compared to the commonly used BOLD techniques, CBF-techniques have poor temporal resolution due to the necessity of an additional inversion-prepared delay and presently their extension to rapidly acquire multislice images to cover the whole brain requires long times.

4. Artifacts

In fMRI studies, only signal changes related to neuronal activity should be observed. However, many other sources contribute to image-to-image intensity fluctuations in consecutively acquired images during the functional mapping study. Signal fluctuation is detrimental to fMRI since it may overwhelm the signal changes related to functional activity. These sources include system instability and subject's movement, as well as normal physiological processes and motions.

4.1. Task-related head motion

Task-related head motions can induce false signal changes in fMRI in high contrast areas (Hajnal et al., 1994) such as the edge of the brain. These problems become more serious when higher spatial resolution is required. To prevent, detect and correct head motions, various approaches have been suggested (Woods et al., 1992; Jezzard and Goldstein, 1994; Chen et al., 1995).

For immobilization of the subject's head, one or a combination of methods such as the use of a vacuum pillow, bite bar, molded foam cast, and a face mask is used in many fMRI laboratories. Since subjects need to stay inside the confined bore of the magnet for a considerable amount of time, comfort as well as motion restrain must be considered. Although some constraint methods (foam cast and face mask) are more effective than others, it is difficult to completely avoid motion problems. Head motion can be monitored by external motion detectors using infrared and pressure sensors (Jezzard and Goldstein, 1994; Chen et al., 1995). Head motions can also be examined directly from the fMRI data using CINE movies and the center of mass approach. Movements of boundaries of the brain and well defined structures within the brain such as the ventricles can be visually identified using CINE. In a more quantitative manner, the center of mass of the images can be calculated and assessed for variations during the study

period. When gross head motion is detected, this can in principle be corrected by registration algorithms; one example of a registration algorithm is that described by Woods et al. (1992), in which the variance of the ratio of voxels in two image sets is minimized by three translations and three rotations. To perform image registration properly, multi-slice or 3-D images are needed. Note, however, that head motion may not just have the effect of rigid body rotation and/or translation on the images acquired. If image distortions exist due to magnetic field inhomogeneities as they do in rapid imaging techniques such as EPI or due to non-linearities in the gradient field profile as is likely for small head gradients, then the head motion will result in alterations of these distortions. Consequently, the effect will not just be a rigid body motion and cannot be corrected simply by rigid-body registration algorithms.

4.2. Physiological motions

Physiological motions include cardiac pulsation and respiration. The chest and the abdomen move due to respiration, affecting the MR signal of the brain significantly (Noll and Schneider, 1994). In order to reduce signal variations in fMRI induced by physiological motions, several approaches have been proposed such as gating (Kupusamy et al., 1995), the navigator echo (Hu and Kim, 1994), digital filtering (Biswal et al., 1996), and retrospective correction (Hu et al., 1995). Data acquisition can also be synchronized to a specific motion by gating when repetition time is sufficiently long as may be for multi-slice whole brain imaging; in this case, gating can be performed so that a given slice will be acquired repeatedly at the same phase of the motion. However, gating must be performed so that image repetition time for a given slice is sufficiently long to permit full relaxation of spins; otherwise, naturally arrhythmic physiological processes such as respiration and cardiac cycle will induce variations in the time interval between consecutive images, leading to intensity variations due to variable relaxation.

A recent technique, based on the navigator echo approach originally proposed for spin-echo imaging (Ehman and Felmlec, 1989), was developed to reduce the motion related noise in conventional (FLASH)-based fMRI images (Hu and Kim, 1994). Navigator echoes were acquired before application of phase-encoding and readout gradients. Signal from the navigator represents the whole imaging slice, and thus monitors global signal modulation, which most likely arises from respiration-related global motion or phase fluctuation. Using the navigator as a reference, this modulation can be corrected for the different phase encoding steps collected during the FLASH image quisition. By this procedure, 30–50% reduction in image-to-image signal fluctuations was attained in gray

and white matter while reduction in the large veins and the cerebrospinal fluid (CSF) were negligible (Hu and Kim, 1994). With this technique, improved functional images were obtained (Hu and Kim, 1994). However, this approach leads to a reduction in image-to-image signal fluctuations indirectly by directly reducing intra-image fluctuations. Therefore, it is not applicable to single-shot echo planar imaging where the fast, single shot approach virtually eliminates intra-image fluctuations.

For EPI, the frequencies corresponding to the cardiac pulsation and respiration can be determined from fMRI data and suppressed by post-processing methods. For example, band-reject filtering (Bandettini et al., 1993; Biswal et al., 1996) can improve the detection of weak signals without increasing the probability of false positives (Biswal et al., 1996). However, for this approach, fMRI data has to be acquired at a frequency faster than physiological frequencies.

Direct monitoring of respiration and cardiac pulsation during the fMRI study and correcting for their effects in fMRI retrospectively (Hu et al., 1995) has also been reported. In this approach, both the respiration and heart beat induced effects are assumed to be pseudo-periodic so that they can be calculated by fitting the repeated measurements of each data point as a function of the phase within the corresponding unit cycle (cardiac or respiration). The estimated respiratory and cardiac effects are removed from the fMRI data without altering task-induced signal changes. Experimental studies performed with FLASH and EPI sequences have demonstrated that the new technique is effective in reducing physiological fluctuation and improving the sensitivity of functional MRI (Hu et al., 1995). Fig. 3 shows the effectiveness of the retrospective method. Clearly, with correction, signal fluctuations related to physiological motions are removed in the time course (Hu et al., 1995).

5. Vasculature considerations

The goal of fMRI is to be able to observe focal changes in image intensity caused by hemodynamic alterations in the local microvascular bed of the gray matter involved in the task. Therefore, the ability to distinguish the macro- versus the micro-vascular effects is of particular importance in functional imaging studies whether they are based on CBF changes only or on the BOLD phenomenon. We can divide the vasculature into two different classes; microvasculature is denoted by arterioles, capillaries and venules which can not be spatially resolved in MR images, while macrovasculature consists of large arteries and veins. If the observed image intensity changes can only be detected in large (macroscopic) vessels which drain/supply the function-

ally involved gray matter regions, then fMRI will be somewhat spatially non-specific for the functionally activated areas. Since vessels of this size be run several cm in length, it becomes difficult to discern the actual gray matter region of increased neuronal activity and effective spatial resolution is degraded. However, there is considerable dilution of deoxyhemoglobin changes downstream from the neuronally active region by blood draining from inactive areas. This reduces the probability of significant contributions from large vessel in BOLD fMRI. Nonetheless, large vessel contributions in both BOLD and CBF-based fMRI should be avoided.

5.1. Separation of macrovascular inflow effects from BOLD effects

BOLD contrast images obtained under rapid RF pulsing conditions can have an 'inflow' component from large vessels (Menon et al., 1993; Lai et al., 1993; Kim et al., 1994a; Duyn et al., 1994; Frahm et al., 1994; Segebarth et al., 1994) that is dominated by fast flowing macrovascular blood in arteries and large veins. This macrovascular inflow effect has probably been the major source of 'activation' in numerous early functional imaging studies conducted with conventional techniques (e.g., FLASH) which used large tip angles and rapid pulsing in order to have adequate SNR. In a conventional linear phase-encoding scheme, the magnetization approaches a steady state governed by the repetition time (TR). Low k-space lines which contribute most of the signal intensity in the image are
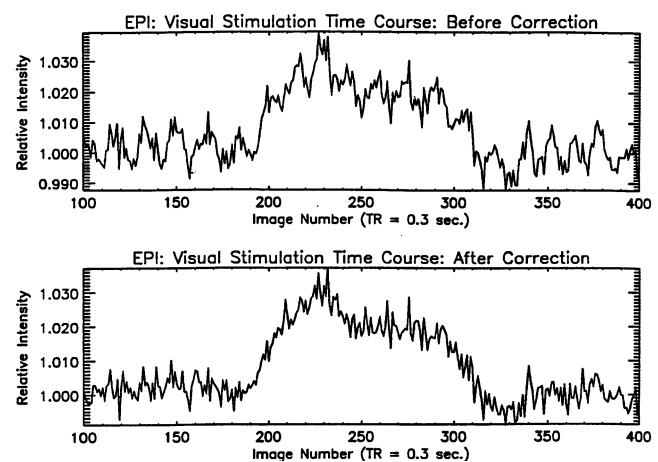

Fig. 3. Time courses of fMRI signal intensity at an activated region in the visual area during visual stimulation, before (top panel) and after (bottom panel) motion correction. The Y axis represents fMRI signal intensity and the X axis represents image numbers. Signal intensities were obtained from BOLD contrast images acquired by the EPI technique with a temporal resolution of 0.3 s. The visual stimulation was performed during images 180–280. In the top panel, physiological oscillations were evident. After correction, these fluctuations are significantly. Thus, the sensitivity of fMRI is improved (Hu et al., 1995). (Kindly provided by Xiaoping Hu).

sampled during a steady state condition; therefore, fresh inflowing spins contribute significantly to image intensity and consequently, increases in macro-vascular flow upon stimulation can give rise to considerable increases in image intensity in the macrovasculature.

This confounding effect, however, can be easily eliminated by allowing full relaxation between images. In single slice EPI, flow sensitivity can be eliminated by pulsing slowly relative to excitation flip angles. In multi-slice EPI images, flow sensitivity due to effects between slices can in principle be still present unless time between acquisition of each slice is sufficiently long to permit full relaxation; this, however, is impractical and thus never performed. Spin-echo based techniques will also reduce inflow effects; signals from stationary tissues will refocus at the spin echo time, while spins of fast moving components may dephase due to altered local inhomogeneities, resulting in loss of signal intensity. A possible solution for suppressing inflow in FLASH is to use a lower RF tip angle relative to TR with a consequent loss in SNR (Frahm et al., 1994). The alternative way is to use a centric phase encoding scheme in which the zero phase-encoding k-space line is acquired first, followed by increasingly higher order k-space values (0, $+1$, -1, $+2$, -2, etc.) (Kim et al., 1994a). Every image is preceded by a several second delay which allows the static and flowing magnetization to recover considerably, thereby reducing the flow sensitivity of the sequence.

5.2. Separation of micro- and macro-vascular BOLD effects

When the 'inflow' component is suppressed, it is possible to specifically examine the vascular origin of the BOLD phenomenon. The BOLD phenomenon has two components (Ogawa et al., 1993a; Weisskoff et al., 1994); one is due to dephasing of the magnetization in the presence of susceptibility-induced gradients of relatively large venous vessels, and the other is due to diffusion within the steep, susceptibility-induced gradients from small vessels (capillaries and venules). The first component induces high percentage signal changes. Generally, areas with some of the most intense stimulation-related signal intensity change lie over large venous vessels (Menon et al., 1993; Kim et al., 1994a; Menon et al., 1995a). This component may have contributed predominantly to the fMRI maps acquired at short TE and/or at low magnetic fields (Menon et al., 1993; Lai et al., 1993; Kim et al., 1994a; Duyn et al., 1994; Frahm et al., 1994; Segebarth et al., 1994). The second component induces small signal changes in diffuse areas which are not associated with any detectable large venous vessels. The BOLD effect in these areas presumably arises from tissues around and inside small vessels (sub-millimeter diameter). Spin-echo images are less sensitive to susceptibility effects in large vessels than gradient-echo images (Ogawa et al., 1993b; Weisskoff et al. 1994). However, the T_2 of blood in large venous vessels is changed during specific tasks (Thulborn et al., 1982; Ogawa et al., 1993b; Bandettini et al., 1995). Therefore, spin-echo or asymmetric spin-echo techniques are not immune to large vessel contributions. Note that images with a higher resolution have a lesser SNR and thus are less sensitive to small changes that arise from the microvasculature.

In BOLD-based fMRI, macro- and micro-vascular components coexist. Thus, specificity of BOLD-based functional location is important. In the motor cortical area, a large Rolandic vein runs along the central sulcus, and each part of the motor cortex controls a different part of the body (Penfield and Boldrey, 1937); thus it is an ideal place to test specificity. Fig. 4 shows functional activation during performance of toe and finger movements (Kim et al., 1994a). Clearly, the finger motor area which is lateral and posterior wall of the precentral gyrus shows activation only during the finger movements, while the medial wall of the motor cortex is activated during the toe movements. These functional activation sites are consistent with the well-known somatotopic maps of the motor cortex (Penfield and Boldrey, 1937).

One approach to minimize intra-vascular components (including micro- and macro-vessels) is to use bipolar gradients (as employed in diffusion-weighted images), which, with a 'b' value of ~ 30 s/mm^2, are expected to leave predominantly an extravascular contribution (Le Bihan et al., 1988; Neil et al., 1991). At high magnetic fields (3 and 4 Tesla), signal changes induced by visual and motor activation were observed even at b values of greater than 200 s/mm^2 and these areas were $\sim 40\%$ of the total activated area determined in the absence of diffusion gradients (Menon et al., 1994; Song et al., 1995). However, task-related signal changes were eliminated at a b value of 42 s/mm^2 at 1.5 T (Song et al., 1994; 1995). These findings suggest that extravascular and intravascular components coexist at high fields. At low fields, the intravascular component dominates the BOLD effect. Thus, to increase BOLD effects at the micro-vascular (including intra and extra-vascular) level, higher magnetic field strengths may be used. The theoretical modeling (Ogawa et al., 1993a; Weisskoff et al., 1994; Bandettini et al., 1995) and preliminary data (Turner et al., 1993; Song et al., 1995; Gati et al., 1995; Song et al., 1995) suggest strongly that higher magnetic fields provide stronger task-induced signal changes. In fMRI, the important parameter is the ratio of the task-induced signal change to signal fluctuation ('contrast-to-noise ratio'; CNR). According to preliminary studies (Jezzard et al., 1993), signal fluctuations of images are not dependent on magnetic field strength. This suggests that higher magnetic fields will provide higher   provided that instrumental problems do not dominate the signal fluctuations.
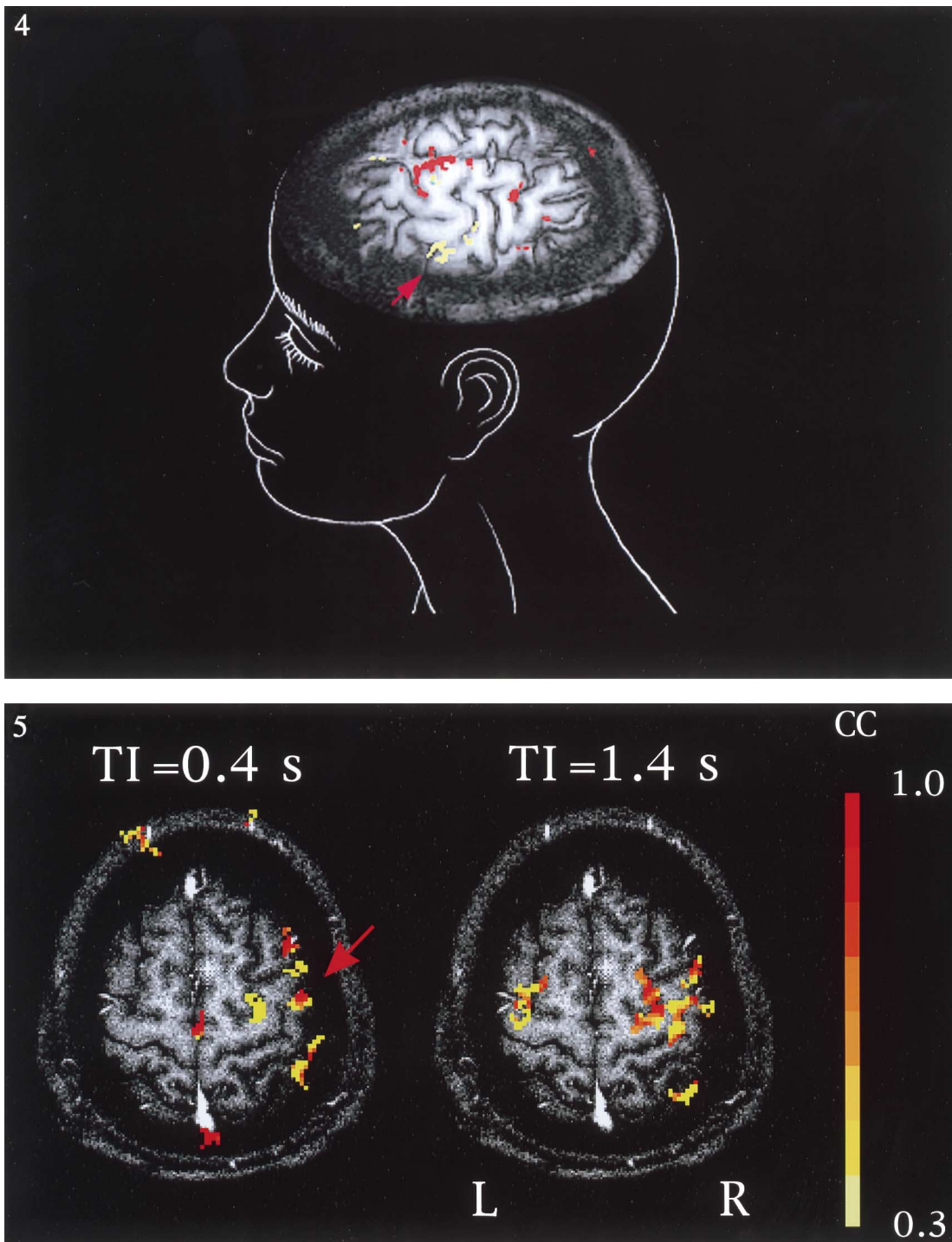
Fig. 4. A BOLD-based functional map during right finger and right toe movements, combined with head sketch. Since an oblique slice was selected along the left central sulcus, the left hemisphere is shown predominantly. An arrow indicates the left central sulcus. Yellow represents functional areas activated only during the finger movements; red, only during the toe movements; and green, during both tasks. (Kim et al., 1994a).

Fig. 5. Blood flow-based FAIR functional maps using inversion times of 0.4 and 1.4 s during left-hand finger opposition movements. Functional maps were generated by a cross-correlation (CC) method using a threshold of cross-correlation value 0.3 ($P < 0.05$). Each color represents a 0.1 cc value increment. In the background image with gray scale, bright areas at the edge of the brain indicate large inflow areas. The FAIR imaging technique was used to acquire 0.4 and 1.4 s IR images in an interleaved fashion. Physiological conditions were identical. Using a short inversion time (i.e., delay time), signal changes were predominantly observed at large inflow areas including the scalp. When the delay time increased to 1.4 s, the signal changes at large vessel areas disappeared. Gray matter areas were mainly seen during movements. A arrow indicates the central sulcus. R, right hemisphere; L, left hemisphere. (Kim, 1995; Kim and Tsekos, 1997).

5.3. Separation of micro- and macro-vascular inflow effects

In T_1-based fMRI techniques, macro- and micro-vascular effects can be differentiated by adjusting the delay time between spin tagging and data collection (i.e., inversion time) (Kim and Tsekos, 1997). Tagged blood proton spins move into the imaging slice through large arterial vessels. Then, they are delivered into capillaries and exchange with tissue water proton spins (perfusion). Depending on the travel distance and inversion time, contributions from macro- and micro-vessels will be different. Complete refreshment of tagged spins occurs when the inversion time is greater than or equal to travel distance/velocity. For example, with a travel distance of 10 mm and flow velocities of greater than 5 cm/s, fresh blood spins will be completely replenished during the inversion time of greater than 0.2 s, regardless of control or stimulation periods. Thus, increases in these flows do not induce significant task related signal changes. CBF-based fMRI maps (FAIR method) with two different inversion times of 0.4 and 1.4 s are shown in Fig. 5. Since both images were acquired during finger opposition in an interleaved manner, changes in physiological parameters are the same. Therefore, differences seen in Fig. 5 are only due to the inversion time. Large inflow areas can be identified as bright spots in the high resolution T_1-weighted image. At a short inversion time, signal changes are located predominantly in large vessels including the scalp; thus, fMRI based on flow changes in large vessels has poor correlation to neuronal activity areas. However, at a long inversion time, these vessel do not contribute to a fMRI map due to complete refreshment, and predominantly microvascular effects are observed. During finger opposition, contralateral motor and bilateral premotor areas were activated. Small, but detectable, blood flow changes were observed at the ipsilateral motor area. In order to reduce the macrovascular contributions in the functional images, a thinner inversion slab and/or a longer inversion time can be used.

6. Limitations of spatial and temporal resolution

Since MRI can in principle be acquired with very high spatial resolution, high resolution functional brain maps can also, in principle, be achieved. The question remains, however, as to what the spatial relationship between neuronal activity and hemodynamic response is. Grinvald and coworkers (Frostig et al., 1990; Grinvald et al., 1991; Turner and Grinvald, 1994) reported that the hemodynamic response area is more spread out than the area of neuronal activation (extending 2–3 mm). This suggests that spatial resolution of an fMRI map is limited by the spatial response of CBF. In optical images, ocular dominance columns of a monkey brain can be mapped using the initial period of deoxyhemoglobin changes (Frostig et al., 1990; Grinvald et al., 1991), suggesting that higher spatial resolution can be obtained when BOLD effects are observed within 2–3 s following stimulation. This initial period is related to oxygen consumption (metabolism) rather than CBF change. Areas based on metabolic changes will be more spatially specific to areas of increased neuronal activity. However, (negative) BOLD signal changes in the initial period are small (Menon et al., 1995a; see also above). Even at 4 T with a surface coil, data from many trials are averaged to obtain the initial negative 'dip'. This demanding measurement may not be used routinely. When a hemodynamic steady state condition (a later time period) is used for fMRI, activated areas may be extended away from areas with neuronal activity. However, these commonly activated areas can be canceled out by comparing fMRI images during two tasks, leaving only areas related to each task. To map ocular dominance columns in humans, Menon et al. (1995b) used right and left eye stimulation alternatively. By comparing two images, the pixels only related to right- or left-eye response were found to be interleaved, perpendicular to the cortical ribbon. The interlaced regions were about 500 μm^2.

Since fMRI images can be obtained in a short time, very high temporal resolution can theoretically be achieved. However, the temporal resolution of fMRI is limited by an intrinsic hemodynamic response time. For example, in an early study, Blamire et al. (1992) observed that maximal fMRI signal changes occurred ~ 6 s following brief visual stimulation periods. Similarly, Bandettini et al. (1993) studied the temporal correlation of fMRI data to task parameters during alternating finger movement and rest periods. A strong correlation was observed when the switching frequency was 0.062 Hz (i.e., 8 s movement and 8 s control), while no correlation was detected with a frequency of 0.125 Hz, suggesting that temporal resolution cannot be better than 8 s. Using high magnetic fields with higher SNR and larger BOLD effects, the temporal resolution of the fMRI signal from the motor area during repeated tasks was found to be about 5 s (Kim et al., 1997).

Temporal resolution in different cortical regions can be examined by offsetting sequential stimuli (Kim et al., 1997). Using a 400 ms repeat time EPI technique and offsetting hemifield stimuli by 500 ms, Savoy et al. (1995) found that the hemodynamic response in the two hemispheres was offset by ~ 500 ms. Dynamic fMRI with high temporal resolution may be useful to study sequential processing of some behavioral tasks such as mental rotation (Shepard and Metzler, 1973), which operates over hundreds of milliseconds to several seconds (et al., 1997). It is recognized that the plethora of neural processes that operate in tens of

milliseconds domain will remain outside the capabilities of fMRI. Note that hemodynamic responses may be different depending on the vascular architecture; the large vessel component may have detectable time-delayed response compared with the small vessel component (Lee et al., 1995).

7. Data processing

From fMRI data, functional maps have to be constructed. Typically signal intensities of images acquired during control and task periods are compared on a pixel-by-pixel basis. Initially, a simple subtraction method has been used for fMRI studies (Bandettini et al., 1992; Kwong et al., 1992; Ogawa et al., 1992). However, if statistical criteria are not used for the decision, the threshold can be arbitrary. Therefore, many statistical approaches have been proposed.

In any statistical test, a significant value needs to be decided on. If the value is chosen too high, one risks to miss the areas with small signal changes (more likely in tissue areas rather than in vessel areas). If the value is too low, fMRI maps may contain many pixels that are not related to tasks. Questions remain as to how to determine a proper threshold value. Since activation is expected to be over several contiguous pixels, a minimum cluster size of activated pixels can also be used for a threshold (Forman et al., 1995). However, the criteria to choose the number of pixels to be contiguous are also arbitrary.

A fractional (percent) signal change map is calculated for pixels which are statistically significant. Although the percent signal changes in BOLD-based functional maps are dependent on slice thickness, resolution, echo time, etc., the average signal change in the volume of interest can provide insight into the origin of activation. For example, a large signal change is likely to originate from a large vessel area (Menon et al., 1993, 1995a), in which case extreme care has to be taken during the analysis of fMRI maps. A higher percent change in tissue areas may not correspond to higher neuronal activity because BOLD effect is based on uncoupling between CBF and OC.

7.1. Student's t-test

One of the most common methods to calculate fMRI maps is to use the parametrical Student's *t*-test. By comparing the ratio of signal difference of the means (in two conditions) to the standard error of the difference of sample means, a significance (P) value is determined. The P value of 0.05 means that five in 100 pixels are statistically significant just by chance. For example, when a matrix size of 64×64 is used for comparison, 204 pixels are statistically significant without any task-

induced signal changes. To minimize false activation, an effectively higher significance value can be used by the Bonferroni correction. The P value of < 0.05 with correction corresponds to a P value of < 0.00001 without correction. However, this is too stringent, and thus modified Bonferroni correction should be used (Worsley et al., 1996). Another way is to use multiple *t* tests with the same pixel when the data set is divided into multiple smaller sets. Only pixels that passed all *t* tests will be used for fMRI maps. In this way, false activation can be completely eliminated (because the likelihood of passing all tests is negligible) and the active pixels are reproducible during repeated tasks. The Student's *t*-test ignores the time dependency of signal intensity, which is a disadvantage as this might be potentially useful.

7.2. Cross-correlation method

Cross-correlation coefficients are calculated between the time course of the pixel intensity and a reference function (Bandettini et al., 1993; Friston et al., 1994). It is assumed that the signal change in the activated area follows the reference function, which is often the stimulation function. The reference function can be the measured time course. One advantage of this method is that the temporal offset in time courses can be determined.

7.3. Spatio-temporal analysis without prior assumptions

The aforementioned techniques need prior knowledge of the brain function. However, this condition may not be fulfilled in a cognitive function, which may not follow simple on-and-off patterns. Temporal responses of different areas may be different. In this case, groups of pixels which behave together may be identified by the principal component analysis (PCA) (Mitra et al., 1997) or fuzzy cluster analysis (Scarth et al., 1995). In PCA, many principal components exist above the random noise level in fMRI data sets; some principal components relate to physiological motions and gross head motion, and a few components relate to tasking. Often it is possible to separate the task-induced activation from motion-related changes. Spatio-temporal dynamics can be determined by using the PCA and cluster analysis. The main disadvantage is that users have to make a decision which component (cluster) should be included in functional maps. It is also not easy to assign statistical significance to any particular components or cluster of pixels found.

8. Conclusions

There are many important areas which can   be covered in this article. In particular, the application of

fMRI to neuroscience is completely omitted. Functional MRI is still in its infancy. At this stage of development, some precautions should be exercised when interpreting fMRI data. Activation sites observed at this stage may be only part of the total area of neuronal activity; using a system with higher sensitivity and improved data processing methods, areas which are not detected with current techniques might be observed. The inevitable additional advances in fMRI techniques will undoubtedly provide a better tool for studying human brain function with high spatial and temporal resolution.

Acknowledgements

References

Bandettini, P.A., Wong, E.C., Hinks, R.S., Tikofsky, R.S. and Hyde, J.S. (1992) Time course EPI of human brain function during task activation, Magn. Reson. Med., 25: 390–398.

Bandettini, P.A., Jesmanowicz, A., Wong, E.C. and Hyde, J.S. (1993) Processing strategies for time-course data sets in functional MRI of the human brain, Magn. Reson. Med., 30: 161–173.

Bandettini, P.A., Boxerman, J.L., Davis, T.L., Wong, E.C., Weisskoff, R.M. and Rosen, B.R. (1995) Numerical simulations of the oxygenation dependence of the T_2 and T_2^* of whole blood using a deterministic diffusion model, Proc. 3rd Soc. Magn. Reson., p. 456.

Belliveau, J.W., Kennedy, D.N., McKinstry, R.C., Buchbinder, B.R., Weisskoff, R.M., Cohen, M.S., Vevea, J.M., Brady, T.J. and Rosen, B.R. (1991) Functional mapping of the human visual cortex by magnetic resonance imaging, Science, 254: 716–719.

Biswal, B., DeYoe, E.A. and Hyde, J.S. (1996) Reduction of physiological fluctuations in fMRI using digital filters, Magn. Reson. Med., 35: 117–113.

Blamire, A., Ogawa, S., Ugurbil, K., et al. (1992) Dynamic mapping of the human visual cortex by high-speed resonance imaging, Proc. Natl. Acad. Sci. USA, 89: 11 060–11 073.

Bowtell, R., McIntyre, D.J.O., Commandre, M.J., Glover, P.M. and Mansfield, P. (1994) Correction of geometric distortion in echo planar images, Proc. 2nd Soc. Magn. Reson., p. 411.

Butts, K., Riederer, S.J., Ehman, R.L., Thompson, R.T. and Jack, C.R. (1994) Interleaved echo planar imaging on a standard MRI system, Magn. Reson. Med., 31: 67–72

Chen, W., Merkle, H., Erhard, P. and Ugurbil, K. (1995) A robust device for monitoring head movement during functional MRI studies, Proc. 3rd Soc. Magn. Reson., p. 747.

Connelly, A., Jackson, G.D., Frankowiak, R.S.J., Belliveau, J.W.,

Vargha-Khadem, F. and Gadian, D.G. (1993) Functional mapping of activated human primary cortex with a clinical MR imaging system, Radiology, 188: 125–130.

Constable, R.T., McCarthy, G., Allison, T., Sanderson, A.W. and Gore, J.R. (1993) Functional brain imaging at 1.5 Tesla using conventional gradient echo imaging techniques, Magn. Reson. Imaging, 11: 451–459.

Detre, J.A., Leigh, J.S., Williams, D.S. and Koretsky, A.P. (1992) Perfusion imaging, Magn. Reson. Med., 23: 37–45.

Duyn, J.H., Moonen, C.T.W., van Yperen, G.H., de Boer, R.W. and Luyten, P.R. (1994) Inflow versus deoxyhemoglobin effects in BOLD functional MRI using gradient echoes at 1.5T, NMR Biomed., 7: 4–9.

Edelman, R.E., Siewer, B., Darby, D.G., Thangaraj, V., Nobre, A.C., Mesulam, M.M. and Warach, S. (1994) Qualitative mapping of cerebral blood flow and functional localization with echo-planar MR imaging and signal targeting with alternating radio frequency, Radiology, 192: 513–520.

Ehman, R.L. and Felmlec, J.P. (1989) Adaptive technique for high-definition MR imaging of moving structures, Radiology, 173: 255–263.

Ellermann, J., Flament, D., Kim, S.-G., Fu, G.F., Merkle, K., Ebner, T.J. and Ugurbil, K. (1994) Spatial patterns of functional activation of the cerebellum investigated using high filed (4T) MRI, NMR Biomed., 7: 63–68.

Ernst, T. and Hennig, J. (1994) Observation of a fast response in functional MR, Magn. Reson. Med., 32: 146–149.

Flament, D., Ellermann, J., Kim, S.-G., Ugurbil, K. and Ebner, T.J. (1997) Functional magnetic resonance imaging of cerebellar activation during the learning of visuo-motor dissociation task, Human Brain Mapping, 4: 210–216.

Forman, S.D., Cohen, J.D., Fitzgerald, M., Eddy, W.F., Mintun, M.A. and Noll, D.C. (1995) Improved assessment of significant activation in functional magnetic resonance imaging (fMRI): use of a cluster-size threshold, Magn. Reson. Med., 33: 636–647.

Fox, P.T. and Raichle, M.E. (1986) Focal physiological uncoupling of cerebral blood flow and oxidative metabolism during somatosensory stimulation in human subjects, Proc. Natl. Acad. Sci. USA, 83: 1140–1144.

Fox, P.T., Raichle, M.E., Mintun, M.A. and Dence, C. (1988) Nonoxidative glucose consumption during focal physiological neural activity, Science, 241: 462–464.

Frahm, J., Bruhn, H., Merboldt, K.D. and Hanicke, W. (1992) Dynamic MRI of human brain oxygenation during rest and photic stimulation, J. Magn. Reson. Imaging, 2: 501–505.

Frahm, J., Merboldt, K.D. and Hanicke, W. (1993) Functional MRI of human brain activation at high spatial resolution, Magn. Reson. Med., 29: 139–144.

Frahm, J., Merboldt, K.D., Hanicke, W., Kleinschmidt, A. and Boecker, H. (1994) Brain and vein—oxygenation or flow? On signal physiology in functional MRI of human brain activation, NMR Biomed., 7: 45–53.

Friston, K.J., Jezzard, P. and Turner, R. (1994) Analysis of functional MRI time-series, Hum. Brain Map., 1: 153–171.

Frostig, R.D., Lieke, E.E., Ts'o, D.Y. and Grinvald, A. (1990) Cortical functional architecture and local coupling between neuronal activity and the microcirculation revealed by in vivo high resolution optical imaging of intrinsic signals, Proc. Natl. Sci., USA, 87: 6082–6086.

Gati, J.S., Menon, R.S., Ugurbil, K. and Rutt, B.K. (1995) Experimental determination of the BOLD field dependence in tissue and vessels, Proc. 3rd Soc. Magn. Reson., p. 771.

Grinvald, A., Frostig, R.D., Siegel, R.M. and Bartfeld, E. (1991) High-resolution optical imaging of functional brain architechture in the awake monkey, Proc. Natl.   USA, 88: 11 559–11 563.

Haase, A., Frahm, J., Hanicke, W. and Merboldt K.-D. (1986)

FLASH imaging: rapid NMR imaging using low flip angle pulses, J. Magn. Reson., 67: 258–266.

Haase, A. (1990) Snapshot FLASH MRI: application to T_1-, T_2-, and chemical shift imaging, Magn. Reson. Med., 13: 77–89.

Hajnal, J.V., Myers, R., Oatridge, A., Schwieso, J.E., Young, I.R. and Bydder, G.M. (1994), Artifacts due to stimulus correlated motion in functional imaging of the brain, Magn. Reson. Med., 31: 283–291.

Hennig, J., Janz, C., Speck, O. and Ernst, T. (1995) Examination of the mechanism of the fast response in functional MR, Proc. 3rd. Soc. Magn. Med., p. 449.

Hinke, R.M., Hu, X., Stillman, A.E., Kim, S.-G., Merkle, K., Salmi, R. and Ugurbil, K. (1993) Magnetic resonance functional imaging of Broca's area during internal speech, Neuroreport, 4: 675–678.

Hu, X. and Kim, S.-G. (1993) A new T_2^* weighting technique for magnetic resonance imaging, Magn. Reson. Med., 30: 512–517.

Hu, X. and Kim, S.-G. (1994) Reduction of physiological noise in functional image using navigator echo. Magn. Reson. Med., 31: 495–503.

Hu, X., Le, T.H., Parrish, T. and Erhard, P. (1995) Retrospective estimation and compensation of physiological fluctuation in functional MRI, Magn. Reson. Med., 34: 210–221.

Jezzard, P., Le Bihan, D., Cuenod, C., Pannier, L., Prinster, A. and Turner, R. (1993) An investigation of the contribution of physiological noise in human functional MRI studies at 1.5 Tesla and 4 Tesla, Proc. 12th Soc. Magn. Reson. Med., p. 1392.

Jezzard, P. and Goldstein, S.R. (1994) A head position monitoring device for use in functional MRI studies, Proc. 2nd Soc. Magn. Reson., p. 658.

Jezzard, P. and Balaban, R.S. (1995) Correction for geometric distortion in echo planar images from Bo field variations, Magn. Reson. Med., 34: 65–73.

Karni, A., Meyer, G., Jezzard, P., Adams, M.M., Turner, R. and Ungerleider, L.G., (1995) Functional MRI evidence for adult motor plasticity during motor skill learning, Nature, 377: 155–158.

Kim, S.-G., Ashe, J., Georgopoulos, A.P., Merkle, K., Ellermann, J.M., Menon, R.S., Ogawa, S. and Ugurbil, K. (1993a) Functional imaging of human motor cortex at high magnetic field, J. Neurophysiol., 69: 297–302.

Kim, S.-G., Ashe, J., Hendrich, K., Ellermann, J.M., Merkle, K., Ugurbil, K. and Georgopoulos AP (1993b) Functional magnetic resonance imaging of motor cortex: Hemispheric asymmetry and handedness, Science, 261: 615–617.

Kim, S.-G., Hendrich, K., Hu, X., Merkle, K. and Ugurbil, K. (1994a) Potential pitfalls of functional MRI using conventional gradient recalled echo techniques, NMR Biomed., 7: 69–74,

Kim, S.-G., Ugurbil, K. and Strick, P.L. (1994b) Activation of a cerebellar output nucleus during cognitive processing, Science, 265: 949–951.

Kim, S.-G. (1995) Quantification of relative blood flow change by flow-sensitive alternating inversion recovery (FAIR) technique: application to functional mapping, Magn. Reson. Med., 34: 293–301.

Kim, S.-G., Hu, X., Adriany, G. and Ugurbil, K. (1996) Fast interleaved echo-planar imaging with navigator: High resolution anatomic and functional images at 4 Tesla, Magn. Reson. Med., 35: 895–902.

Kim, S.-G., Richter, W. and Ugurbil, K. (1997) Limitations of temporal resolution in functional MRI, Magn. Reson. Med., 37: 631–636.

Kim, S.-G. and Tsekos, N.V. (1997) Perfusion imaging by a flow-senitive alternating inversin recovery (FAIR) technique: Application to functional brain imaging, Magn. Reson. Med., 37: 425–435.

Kupusamy, K., Lin, W. and Haacke, E.M. (1995) Importance of EKG gating in functional magnetic resonance imaging of human motor cortex, Abs. Soc. Neurosci., p. 1420.

Kwong, K.K., Belliveau, J.W., Chesler, D.A., Goldberg,.I.E., Weisskoff, R.M., Poncelet, B.P., Kennedy, D.N., Hoppel, B.E., Cohen, M.S., Turner, R., Cheng, H.M., Brady, T.J. and Rosen, B.R. (1992) Dynamic magnetic resonance imaging of human brain acrivity during primary sensory stimulation, Proc. Natl. Acad. Sci. USA, 89: 5675–5679.

Lai, S., Hopkins, A.L., Haacke, E.M., Li, D., Wasserman, B.A., Buckley, P., Friedman, L., Meltzer, H., Hedera, P. and Friedland, R. (1993) Identification of vascular structures as a major source of signal contrast in high resolution 2-D and 3-D functional activation imaging of the motor cortex at 1.5T: preliminary results, Magn. Reson. Med., 30: 387–392.

Lauterbur, P.C. (1973) Image formation by induced local interaction: examples employing nuclear magnetic resonance imaging, Nature, 241: 190–191.

Le Bihan, D., Breton, E., Lallemand, D., Aubin, M.L., Vignaud, J. and Laval-Jeantet, M. (1988) Separation of diffusion and perfusion in intravoxel incoherent motion MR imaging, Radiology, 168: 497–505.

Lee, A.T., Glover, G.H. and Meyer, C.H. (1995) Distribution of large venous vessels in time-course spiral blood-oxygen-level-dependent magnetic resonance functional neuroimaging, Magn. Reson. Med., 33: 745–754.

Mansfield, P. (1977) Multi-planar image formation using NMR spin echoes, J. Phys. C, 10: L55–L58.

McCarthy, G., Blamire, A.M., Rothman, D.L., Gruetter, R. and Shulman, R.G. (1993) Echo-planar MRI studies of frontal cortex activation during word generation in humans, Proc. Natl. Acad. Sci. USA, 90: 4952–4956.

Menon, R., Ogawa, S., Kim, S.-G., Ellermann, J.M., Merkle, K., Tank, D.W. and Ugurbil, K. (1992) Functional brain mapping using magnetic resonance imaging signal changes accompanying visual stimulation, Invest. Radiol., 27: S47–S53.

Menon, R.S., Ogawa, S., Tank, D. and Ugurbil, K. (1993) 4 Tesla gradient recalled echo characteristics of photic stimulation induced signal changes in the human primary visual cotex, Magn. Reson. Med., 30: 380–386.

Menon, R.S., Hu, X., Adriany, G., Petersen, P., Ogawa, S. and Ugurbil, K. (1994) Comparison of spin-echo EPI, asymmetric spin-echo EPI and conventional EPI applied to functional neuroimaging: the effect of flow crushing gradients on the BOLD signal, Proc. 2nd Soc. Magn. Reson., p. 622.

Menon, R.S., Ogawa, S., Strupp, J.S., Andersen, P. and Ugurbil, K. (1995a) BOLD-based functional MRI at 4 Tesla includes a capillary bed contribution: echo-planar imaging correlates with previous optical imaging using intrinsic signals, Magn. Reson. Med., 33: 453–459.

Menon, R.S., Ogawa, S., Strupp, J.P. and Ugurbil, K. (1995b) Evidence for human ocular dominance columns mapped using sub-millimeter resolution FLASH, Proc. 3rd Soc. Magn. Reson., p. 163.

Mitra, P.P., Thomson, D.J., Ogawa, S., Hu, X. and Ugurbil, K. (1997) The nature of Spatiotemporal changes in cerebral hemodynamics as manifested in functional magnetic resonance imaging, Magn. Reson. Med., 37: 511–518.

Moonen, C.T.W., Liu, G., van Gelderen, P. and Sobering, G. (1992) A fast gradient-recalled MRI technique with increased sensitivity to dynamic susceptibility effects, Magn. Reson. Med., 26: 184.

Neil, J.J., Scherrer, L.A. and Ackerman, J.J.H. (1991) An approach to solving the dynamic range problem in measurement of the pseudodiffusion coeffient in vivo with spin echoes, J. Magn. Reson., 95: 607–614.

Noll, D.C. and Schneider, W. (1994) Respiration artifacts in functional brain imaging: sources of signal variation and compensation Proc. 2nd Soc. Magn. Reson., p. 647.

Ogawa, S. and Lee, T.M. (1990) Magnetic resonance imaging of

blood vessels at high fields: in vivo and in vitro measurments and image simulation, Magn. Reson. Med., 16: 9–18.

Ogawa, S., Lee, T.M., Nayak, A.S. and Glynn, P. (1990a) Oxygenation-sensitive contrast in magnetic resonance image of rodent brain at high magnietic fields, Magn. Reson. Med., 14: 68–78.

Ogawa, S., Lee, T.M., Kay, A.R. and Tank, D.W. (1990b) Brain magnetic resonance imaging with contrast dependent on blood oxygenation, Proc. Natl. Acad. Sci. USA, 87: 9868–9872.

Ogawa, S., Tank, D., Menon, R., Ellermann, J.M., Kim, S.-G., Merkle, K. and Ugurbil, K. (1992) Intrinsic signal changes accompanying sensory stimulation: functional brain mapping using MRI, Proc. Natl. Acad. Sci. USA, 89: 5951–5955.

Ogawa, S., Menon, R.S., Tank, D., Kim, S.-G., Merkle, K., Ellermann, J.M. and Ugurbil, K. (1993a) Functional brain mapping by blood oxygenation level-dependent contrast magnetic resonance imaging: a comparison of signal characteritics with a biophysical model, Biophys. J., 64: 803–812.

Ogawa, S., Lee, T.M. and Barrere, B. (1993b) The sensitivity of magnetic resonance image signals of a rat brain to changes in the cerebral venous blood oxygenation, Magn. Reson. Med., 29: 205–210.

Pauling, L. and Coryell, C.D. (1936) The magnetic properties and structure of hemoglobin, oxyhemoglobin, and carbonmonoxyhemoglobin, Proc. Natl. Acad. Sci. USA, 22: 210–216.

Penfield, W. and Boldrey, E. (1937) Somatic motor and sensory representation in the cerebral cortex of man as studied by electrical stimulation, Brain, 60: 389–443.

Raichle, M.E. (1987) Circulatory and metabolic correlates of brain function in normal humans. In Mountcastle V.B. and Plum F. (Eds), Handbook of Physiology. The Nervous System, Higher Functions of the Brain. American Physiological Society, Bethesda, pp. 643–674.

Rao, S.M., Binder, J.R., Bandettini, P.A., Hammeke, T.A., Yetkin, F.Z., Jesmanowitz, A., List, L.M., et al. (1993) Functional magnetic resonance imaging of complex human movements, Neurology, 43: 2311–2318.

Richter, W., Andersen, P.M., Georgopoulos, A.P. and Kim, S.-G. (1997) Sequential activity in human motor areas during a delayed cued finger movement task studied by time-resolved fMRI, NeuroReport, 8, in press.

Roberts, D.A., Detre, J.A., Bolinger, L., Insko, E.K. and Leigh, J.S. (1994) Quantitiative magnetic resonance imaging of human brain perfusion at 1.5 T using steady–state inversion of arterial water, Proc. Natl. Acad. Sci. USA, 91: 33–37.

Roland, P.E., Eriksson, L., Stone-Elander, S. and Widen, L. (1987) Does mental activity change the oxidative metabolism of the brain?, J. Neursoci., 7: 2373–2389.

Rosen, B.R., Belliveau, J.W., Arnon, H.J., Kennedy, D., Buchbinder, B.R., Fischman, A., Gruber, M., Glas, J., Weisskoff, R.M., Cohen, M.S., Hochberg, F.H. and Brady, T.J. (1991) Susceptibility contrast imaging of cerebral blood volume: human experience, Magn. Reson. Med., 22: 293–299.

Roy, C.S. and Sherrington, C.S. (1890) On the regulation of blood supply of the brain, J. Physiol., 11: 85–108.

Rzedzian, R.R. and Pykett, I.L. (1987) Instant images of the human heart using a new, whole-body MR imaging system, Am. J. Roentgenol., 149: 245.

Sane, J.N., Donoghue, J.P., Thangaraj, V., Edelman, R.R. and Warach, S. (1995) Shared neural substrates controlling hand movements in human motor cortex, Science, 268: 1775–1777.

Savoy, R.L., Bandettini, P.A., O'Craven, K.M., Kwong, K.K., Davis, T.L., Baker, J.R., Belliveau, J.W., Weisskoff, R.M. and Rosen, B.R. (1995) Pushing the temporal resolution of fMRI: studies of very brief visual stimuli, onset variability and asynchrony, and stimulus-correlated changes in noise, Proc. 3rd Soc. Magn. Reson., p. 450.

Scarth, G., McIntyre, M., Wowk, B. and Somorjai, R. (1995) Detection of novelty in functional images using fuzzy clustering, Proc. 3rd Soc. Magn. Reson., p. 238.

Schneider, W., Noll, D.G. and Cohen, J.G. (1993) Functional topographic mapping of the cortical ribbon in human vision with conventional MRI scanners, Nature, 365: 150–153.

Segebarth, S., Belle, V., Delon, C., Massarelli, R., Decety, J., Le Bas, J.-F., Decorps, M. and Benabid, A.L. (1994) Functional MRI of the human brain: predominance of signals from extracerebral veins, Neuroreport, 5: 813–816.

Seitz, R.J. and Roland, P.E. (1992) Vibratory stimulation increases and decreases the regional cerebral blood flow and oxidative metabolism: a positron emission tomography (PET) study, Acta Neurol. Scand., 86: 60–67.

Sereno, M.I., Dale, A.M., Reppas, J.B., Kwong, K.K., Belliveau, J.W., Brady, T.J., Rosen, B.R. and Tootell, R.B.H. (1995) Borders of multiple visual areas in humans revealed by functional magnetic resonance imaging, Science, 268: 889–893.

Shaywitz, B.A., Shaywitz, S.E., Pugh, K.R., Constable, T.D., Skudlarski, P., Fulbright, R.K., Bronen, R.A., Fletcher, J.M., Shankweiler, D.P., Katz, L. and Gore, J.C. (1995) Sex differences in the functional organization of the brain for language, Nature, 373: 607–609.

Shepard, R.N. and Metzler, J. (1973) Mental rotation of three-dimensional objects, Science, 171: 701–703.

Song, A.W., Wong, E.C., Bandettini, P.A. and Hyde, J.S. (1994) The effect of diffusion weighting on the task-induced functional MRI, Poc. 2nd Soc. Magn. Reson., p. 743.

Song, A.W., Wong, E.C., Jemanowitz, A., Tan, S.G. and Hyde, J.S. (1995) Diffusion weighted fMRI at 1.5T and 3T, Proc. 2nd Soc. Magn. Reson., p. 457.

Stehling, M.K., Turner, R. and Mansfield, P. (1991) Echo-planar imaging: magnetic resonance imaging in a fraction of a second, Science, 254: 53–50.

Talairach, J. and Tournoux, P. (1988) Co-planar Stereotaxic Atlas of the Human Brain, Thieme Med. Pub., New York.

Thulborn, K.R., Waterton, J.C., Mattews, P.M. et al. (1982) Dependence of the transverse relaxation time of water protons in whole blood at high field, Biochem. Biophys. Acta, 714: 265–272.

Turner, R., Le Bihan, D., Moonen, C.T., Despres, D. and Frank, J. (1991) Echo-planar time course MRI of cat brain oxygenation changes, Magn. Reson. Med., 22: 159–166.

Turner, R., Jezzard, P., Wen H, Kwong, K.K., Le Bihan, D., Zeffiro, T. and Balaban, R.S. (1993) Functional mapping of the human visual cortex at 4 and 1.5 Tesla using deoxygenation contrast EPI, Magn. Reson. Med., 29: 277–279.

Turner, R. and Grinvald, A. (1994) Direct visualization of patterns of deoxyhemoglobin and reoxygenation in monkey cortical vasculature during functional brain activation, Proc. 2nd Soc. Magn. Reson. Med., p. 430.

Weisskoff, R.M., Zuo, C.S., Boxerman, J.L. and Rosen, B.R. (1994) Microscopic susceptibility variation and transverse relaxation: theory and experiment, Magn. Reson. Med., 31: 601–610.

Williams, D.S., Detre, J.A., Leigh, J.S. and Koresky, A.P. (1992) Magnetic resonance imaging of perfusion using spin inversion of arterial water, Proc. Natl. Acad. USA, 89: 212–216.

Woods, R.P., Cherry, S.R. and Mazziotta, J.C. (1992) Rapid automated algorithm for aligning and re-slicing PET images, J. Comput. Assisted Tomogr., 16: 620–633.

Worsley, K.J., Marrett, S., Neelin, P., Vandal, A.C., Friston, K.J. and Evans, A.C. (1996) A unified statistical approach for determining significant signals in images of   activation, Human Brain Mapping, 4: 58–73.